Selection of optimum fractal model for detection of stream sediments anomalies

Shiva Shahsavar[1], Ali Reza Jafari Rad[1]*, Peyman Afzal[2], Nima Nezafati[1]
[1] *Department of Geology, Science and Research Branch, Islamic Azad University, Tehran, Iran*
[2] *Department of Petroleum and Mining Engineering, South Tehran Branch, Islamic Azad University, Tehran, Iran*
**Corresponding author, e–mail: alirad@yahoo.com*
(*received: 12/12/2019 ; accepted: 06/04/2020*)

Abstract

The main purpose of this research is a comparative study among four different fractal models including Concentration-Perimeter/Area (C-P/A), Concentration-Number (C-N), Concentration-Area (C-A) and Concentration-Perimeter (C-P) for delineation of stream sediments Au anomalies based on catchment basins in Aghkand region, NW Iran. In this study, a total of 920 stream sediment samples were utilized to determine the geochemical anomalies of Au using the fractal models for selection of optimum model. As a result, the Au anomalies were correlated with geological units located in the western and SW parts of the region that mainly consist of andesite rocks and tuffs. To certify this, 78 litho-geochemical sets of data were utilized to validate the C–P/A, C–N, C–A and C–P fractal models for Au by logratio matrix. The overall accuracy rates are 0.97, 0.96, 0.95 and 0.95 for the C– P/A, C–N, C–A, C–P fractal models, respectively. It showed that the C–P/A model was the optimum fractal model in the study region.

Keywords: *Fractal Models; Stream Sediments; Aghkand.*

Introduction

Separating the geochemical anomalies from their background is among the major goals for recognition and explanation of different ore formation processes (Carranza, 2008; Pirajno, 2009). The selection of an optimum method for anomalies' detection is vital for different cases. Conventional methods consist of statistical methods that have been being used for decades and it was assumed that such methods that have been used for recognition of anomalies were the only applicable cases where geochemical data followed a normal or log-normal distribution and neglected its spatial variability (Davis, 2002). Furthermore, conventional statistical methods contain disadvantages such as normalization of raw data. As a result, conventional methods were gradually replaced by modern methods like fractal/multi-fractal methods (Agterberg, 1995; Cheng *et al*., 2000; Shen & Zhao, 2002; Afzal *et al*., 2010). Fractal/multifractal methods were initially proposed by Cheng *et al*. (1994) and has been applied in geochemical exploration since 1990s (e.g., Cheng *et al*., 1994, 1995; Sim *et al*., 1999; Li *et al*., 2003; Carranza, 2009; Afzal *et al*., 2011, 2012; Sadeghi *et al*., 2015; Zuo *et al*., 2015; Chen & Cheng, 2016; Parsa *et al*., 2016, 2017; Ghezelbash *et al*., 2019a). Some practical fractal models for geochemical exploration include Number-Size (N-S; Mandelbrot, 1983), Concentration-Perimeter/Area (C-P/A; Bölviken *et al*., 1992), Concentration-Area (C-A; Cheng *et al*., 1994), Perimeter-Area (P-A; Cheng, 1995), Spectrum-Area (S-A; Cheng *et al*., 2000), Concentration-Distance (C-D; Li *et al*., 2003), Concentration-Volume (C-V; Afzal *et al*., 2011), Spectrum-Volume (S-V; Afzal *et al*., 2012) and Concentration-Number (C-N; Sadeghi *et al*., 2012; Afzal *et al*., 2016).

Geochemical exploration based on stream sediment data is an efficient method for identification of anomalous areas (Carranza, 2010; Yousefi *et al*., 2012, 2013). Geochemical landscapes have been modeled from point data of stream sediment chemical compositions by creating maps with point symbols contours (Govett, 1983), sample catchment basins (Bonham-Carter, 1994; Bonham-Carter & Goodfellow, 1984, 1986; Carranza, 2010; Carranza & Hale, 1997; Moon, 1999; Spadoni *et al*., 2004), stream orders (Carranza, 2004), and extended sample catchment basins (Spadoni, 2006). In this research, catchment basins of stream sediment samples were developed through digital elevation model (DEM) and were classified after applying the C-P/A, C-N, C-A and C-P fractal models (Ghezelbash *et al*., 2019b). Following that, the results were correlated with geological units. Based on logratio matrix and lithogeochemical samples, the results derived by these models were compared and the appropriate method for delineation of the Au geochemical anomalies in the Aghkand region, NW Iran was selected.

Methodology

Concentration-Area (C-A) fractal model

Cheng *et al*. (1994) developed the C–A fractal model for the definition of geochemical anomalies from the background. The C-A fractal model has the following general form:

$$A(\rho \le \upsilon) \propto \rho^{-a1};\; A(\rho \le v) \propto \rho^{-a2} \quad (1)$$

where A (ρ) denotes the areas that have the concentration values smaller or greater than the contour value ρ, υ stands for the threshold; a1 and a2 are the characteristic exponents that represent fractal dimension. Threshold values in the model represent the boundaries between different geochemical anomalies and zones (Afzal *et al*., 2010, 2014, 2016; Heidari *et al*., 2013, Ghezelbash *et al*., 2019).

Concentration-Perimeter (C-P) fractal model

This model was proposed by Cheng (1995) and has been utilized to indicate the geochemical anomalies from the background with the following form:

$$P(\ge \rho) \propto F\rho^{-\beta} \quad (2)$$

where ρ and P (≥ρ) represent elemental concentration and the perimeter that has concentration values greater than or equal to ρ, respectively. F and β are the constant and the fractal dimension of the distribution of elemental concentrations, respectively (Afzal *et al*., 2016).

Concentration-number (C-N) fractal model

Sadeghi *et al*. (2012) proposed the C-N fractal model in accordance with Number-Size (N-S) fractal model which was proposed by Mandelbrot (1983). It makes a reverse relation between each concentration and cumulative frequency (Mandelbrot, 1983; Sadeghi *et al*., 2012; Afzal *et al*., 2016). This model has the common form as follow:

$$N(\ge C) \propto F\rho^{-\beta} \quad (3)$$

Where N (≥ρ) shows the elemental concentration and the cumulative number of samples which have concentration values greater than ρ value. F is the constant and β is the fractal dimension of the distribution for elemental concentrations. This model uses all initial data without changing the raw data (Deng *et al*., 2010; Afzal *et al*., 2016).

Geological Setting

The Agkhand region is located in the SE of Eastern Azerbaijan province, NW Iran, with an approximate extent of 2920 km^2. It is situated at the intersection of western Alborz, central Iran structural zones and partly Urumieh-Dokhtar magmatic belt (UDMB; Fig. 1). The UDMB hosts many porphyry, epithermal and related types of ore deposits (Atapour & Aftabi, 2007; Shafiei *et al*., 2009; Dargahi *et al*., 2010; Asadi *et al*., 2014; Zarasvandi *et al*., 2015). However, there are various kinds of gold mineralization including intrusion-related, Au-rich VMS, Carlin-like, epithermal and orogenic, especially in NW Iran (Maghsoudi *et al*., 2005; Aliyari *et al*., 2009; Tajeddin, 2011; Heidari *et al*., 2013; Makovicky *et al*., 2013). The continental collision between Iranian microcontinent and the Afro-Arabian continent during closure of the Tethys Ocean in the Late Cretaceous led to the development of a volcanic arc in northwestern Iran (Mohajjel & Fergusson, 2000; Babaie *et al*., 2001; Karimzadeh-Somarin, 2005; Karimzadeh-Somarin & Lentz, 2008). Then, the subduction-related granitic intrusions were emplaced into the volcanic arc during Cenozoic, especially Oligocene and Miocene, Cu–Mo–Au porphyry and epithermal gold mineralization were formed (Hezarkhani & Williams-Jones 1998; Karimzadeh-Somarin & Lentz, 2008). The existence of hydrothermal gold mineralization in some of volcanic-dominated sequences in northwestern Iran (Karimzadeh-Somarin & Lentz, 2008) illustrates the abundance of such hydrothermal systems (Ellis, 1979; Karimzadeh-Somarin & Lentz, 2008).

The oldest rocks in the region belong to Precambrian and Paleozoic which exist in the western part of the region. Precambrian rock types are composed of various metamorphic rocks including metapelites, metabasites, calc-silicates and meta-ultramafic rocks. Paleozoic rock units consist of metamorphic ophiolitic rocks, gneiss, amphibolite, shale and sandstone with interbedded dolomitic limestone. They were metamorphosed to the green schist and granulite facies. The Mesozoic rocks are mostly related to Triassic and Jurassic are located in the western part of the region including dolomitic limestone, siltstone, sandstone, claystone, shale and marl (Fig. 1).

There also exist various Oligocene volcano-plutonic rocks including andesite, trachy-andesite, granodiorite, and granite. There are also some Eocene sedimentary rocks consist of marl, siltstone, limestone, and sandstone (Fig. 1). The region's majority rock types consist of Eocene volcanic and volcano-sedimentary rocks including ignimbrite and tuff. Many researchers have come to the conclusion that these masses are the granitoids of type-I. There also existmany metallic deposits and occurrences that contain Cu, Au, Pb and Zn.

Alluvial terraces, river deposits, low gravel fans and travertine are seen as Quaternary units in the region (Karimzadeh-Somarin, 2006).

There are several metallic and related industrial mineral occurrences or deposits such as copper, gold, barite, iron and kaolinite.

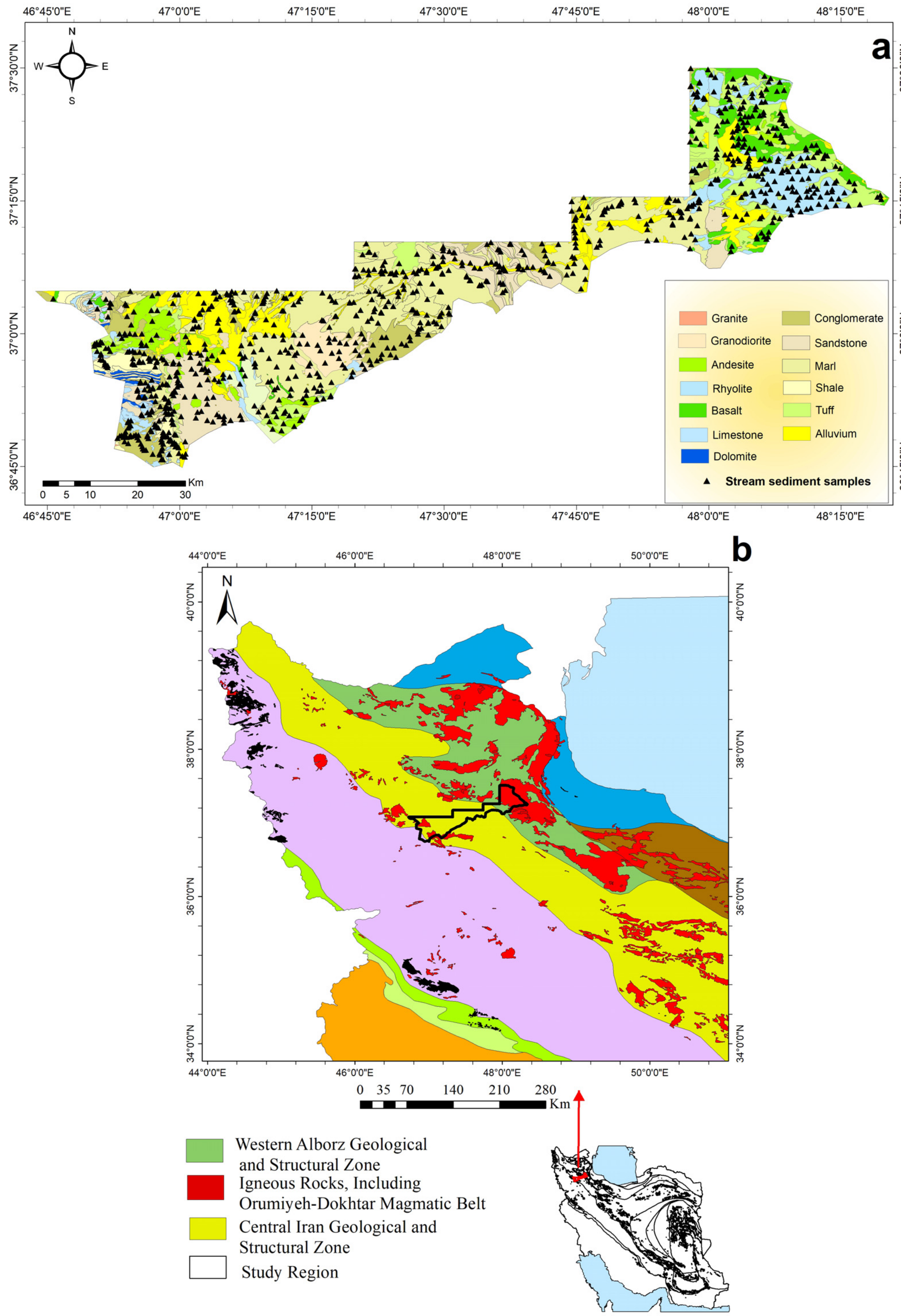

Figure 1. Location of study region in Iran's structural map (based on Sahandy 2006), and simplified geological map with stream sediment location.

Baycheh Baq polymetallic deposit is located in the SE part of the study region which is within the volcano-plutonic rocks of the UDMB. There are Au-Cu-Pb-Zn-Ag mineralization within silisic, argillic and propylitic alteration zones. Moreover, volcanosedimentary and volcanic rocks host metallic mineralization, especially Au (Lotfi & Karimi, 2004). Iron oxides and argillic alteration zones extended in the study region, especially in the western and southwestern parts of Aghkand region. Furthermore, silicification occurs in the region, specifically in the western and SW parts near to Zarshuran Carlin-like deposit. Evidence show that Au mineralization can be epithermal or carlin-like types.

Geochemical data and elemental correlations

In the present study, 920 stream sediment samples along with 78 lithogeochemical samples as a validation were collected and then analyzed via ICP-MS in the laboratory of the Geological Survey of Iran (GIS) for 44 elements. The detection limit for Au is 1 ppb which is important for the correction of censored data. Assay quality assurance (QA) and quality control (QC) were carried out based on 15 duplicate samples. Based on T-student and Fisher tests, there were no meaningful differences and mistakes.

Discussion

The location map for the geochemical samples is represented in Fig. 1. As statistical parameters indicate, Au mean value is 1.31 ppb and the distribution of Au is not normal (Table 1 and Fig. 2). If Au median is assumed equal to the threshold values, then the achieved elemental threshold value is 1.3 ppb for Au, as illustrated in (Table 1). The data was transformed by Ln transformation and its histogram is near to normal distribution (Fig. 3).

Threshold values (break points) for separating geochemical populations were obtained from C-P/A, C-N, C-A and C-P log-log plots which indicate geochemical differences.

Table1. Raw data Statistical parameters according to the analysis of steam sediment samples.

Statistical parameter	Au (ppb)
Mean	1.31
Median	1.3
SD	1.30
Maximum	7.85
Minimum	0.0
SD: standard deviation	

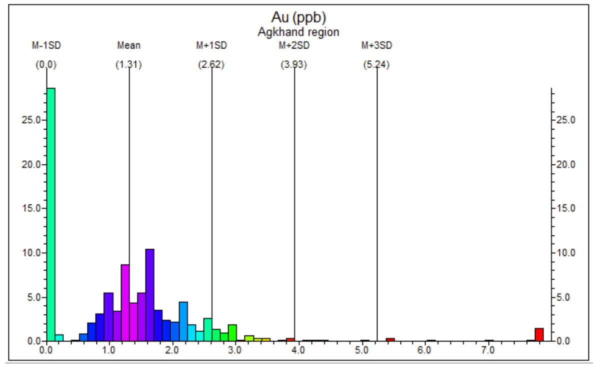

Figure 2. Au histogram according to the stream sediment samples.

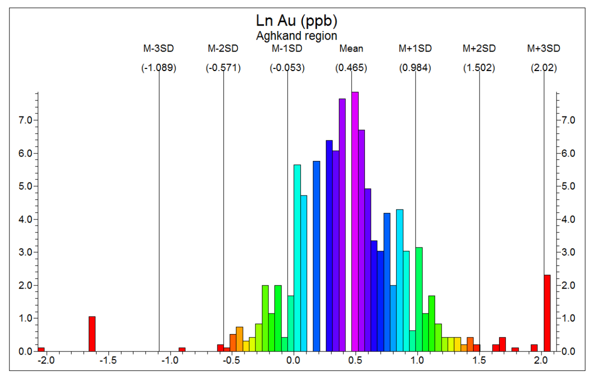

Figure 3. Ln Au histogram according to the stream sediment samples.

According to log-log plots, five geochemical populations can be considered for Au which are obtained by the C-N, C-A and C-P, as can be seen in Fig. 4. The C-P/A log-log plot shows a different result for six populations for Au. Furthermore, the results derived via the C-A and C-P fractal models are analogous (Table 2 and Fig. 5).

Table 2. Au thresholds based on the C–P/A, C–N, C–A, C–P.

Methods	Low-intensity Threshold Au (ppb)	High-intensity Threshold Au (ppb)
C-P/A	0.001	25.1
C-N	1.58	6.91
C-A	0.001	39.8
C-P	0.003	39.8

The geochemical maps for each method were generated using sample catchment basin by ArcGIS 9.3 (Fig. 5). The sample catchment basins of stream sediments were produced from Digital Elevation Model (DEM). Then C-P/A, C-N, C-A, and C-P fractal models were evaluated.

As it is illustrated in Fig. 5, main anomalies for Au happens in the western and southwestern parts of the study region for all fractal models and high intensive anomalies contain Au values >7.9 ppb, >5.2 ppb, >4 ppb and >4 ppb based on the C-P/A, C-N, C-A and C-P, respectively. In addition, the maps of C-A and C-P fractal models are very similar to high intensive anomalies. The maps derived via the C-P/A and C-N indicate different Au anomalies, but there are good correlations between these fractal models. Based on the Au maps, main Au anomalies exist in the western and SW parts of this region (Fig. 5). These anomalies are associated with andesite rocks and tuffs.

Correlation between fractal modeling with lithogeochemical data

The Au anomalies obtained by the fractal models were correlated with lithogeochemical samples using logratio matrix. Carranza (2011) proposed a method for the calculation of spatial correlations between two mathematical models. An intersection operation between major Au anomalies achieved by the various fractal models and concentrated lithogeochemical data was carried out to calculate voxels with respect to each of the overlap zones' four classes as presented in Table 3. Based on the gained numbers of voxels, the overall accuracy (OA), Type I error (T1E) and Type II error (T2E) of geochemical data corresponding to the C–P/A, C–N, C–A and C–P fractal models were calculated.

First, lithogeochemical data were classified using the C-N fractal model. Its log-log plot shows that there are six populations for Au (Fig. 6). Moreover, high intensive lithogeochemical anomalies commence from 446 ppb for Au.

This lithogeochemical samples and logratio matrix can be used for validation of high value of stream sediments anomalies of Au obtained by the C–P/A, C–N, C–A and C–P fractal models.

Table 3. Matrix of comparing performance for the C–P/A, C–N, C–A and C–P fractal modeling results based on stream sediments with high intensive lithogeochemical anomalies (Carranza, 2011).

High Intensive Anomalies Obtained by the C–P/A, C–N, C–A, C–P Fractal Models	**High Intensive Lithogeochemical Anomalies**	
	Inside Anomaly	Outside Anomaly
Inside Anomaly	True positive (A)	False positive (B)
Outside Anomaly	False negative (C)	True negative (D)
	Type I error = C/(A+C)	Type II error = D/(B+D)
	Overall accuracy = (A+D)/(A+B+C+D)	

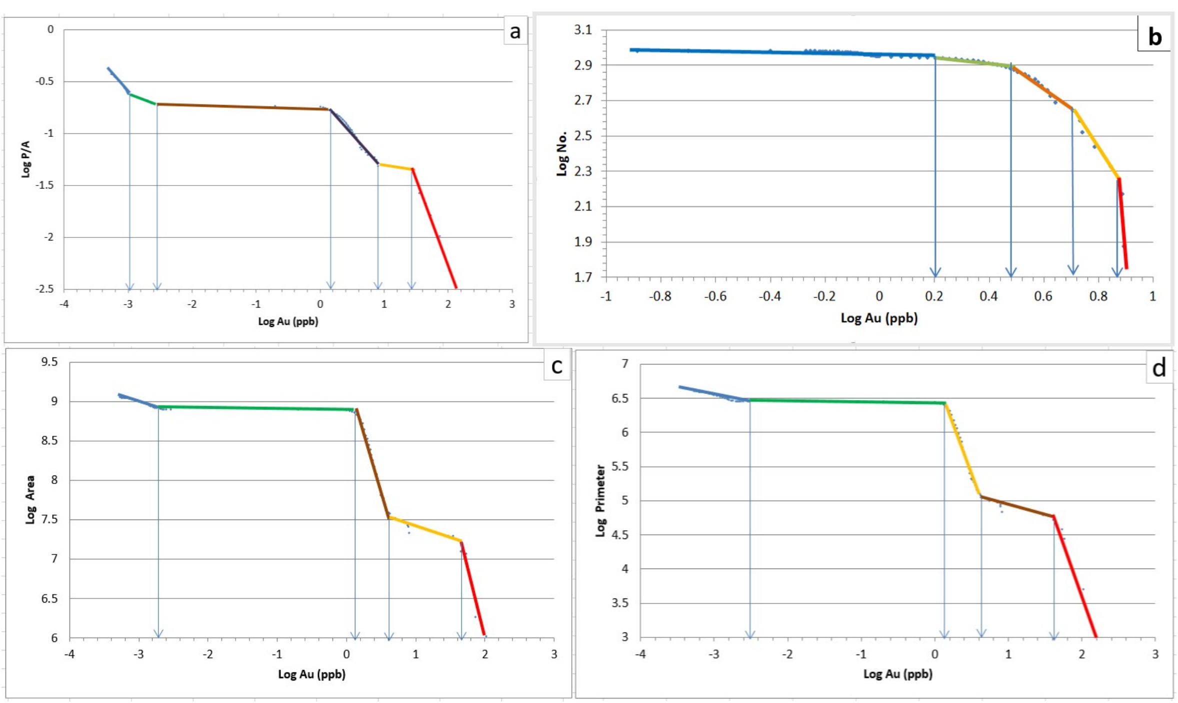

Figure 4. Log-log plots for C-P/A, C-N, C-A and C-P fractal models.

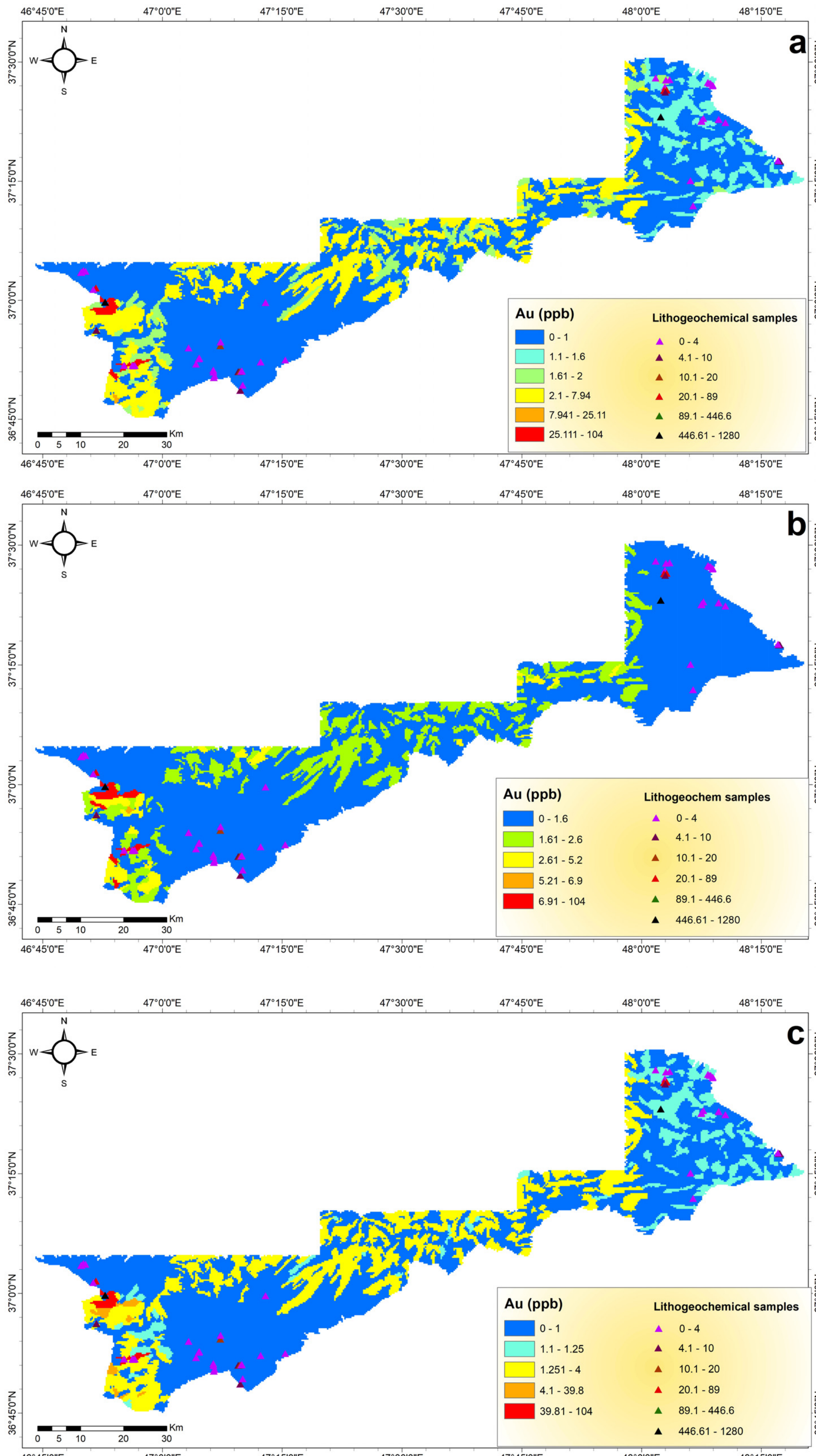
a
Au (ppb)
0 - 1
1.1 - 1.6
1.61 - 2
2.1 - 7.94
7.941 - 25.11
25.111 - 104
Lithogeochemical samples
0 - 4
4.1 - 10
10.1 - 20
20.1 - 89
89.1 - 446.6
446.61 - 1280
b
Au (ppb)
0 - 1.6
1.61 - 2.6
2.61 - 5.2
5.21 - 6.9
6.91 - 104
Lithogeochem samples
0 - 4
4.1 - 10
10.1 - 20
20.1 - 89
89.1 - 446.6
446.61 - 1280
c
Au (ppb)
0 - 1
1.1 - 1.25
1.251 - 4
4.1 - 39.8
39.81 - 104
Lithogeochemical samples
0 - 4
4.1 - 10
10.1 - 20
20.1 - 89
89.1 - 446.6
446.61 - 1280
46°45'0"E
47°0'0"E
47°15'0"E
47°30'0"E
47°45'0"E
48°0'0"E
48°15'0"E
37°30'0"N
37°15'0"N
37°0'0"N
36°45'0"N
Km
0 5 10 20 30

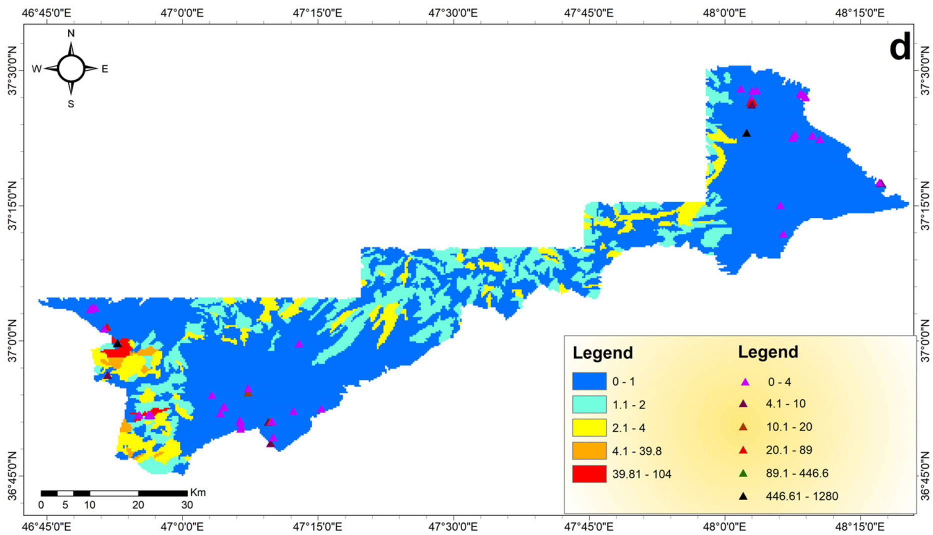

Figure 5. Geochemical maps of the distribution of Au by using C–P/A (a), C–N(b), C–A (c) and C–P (d) fractal models.

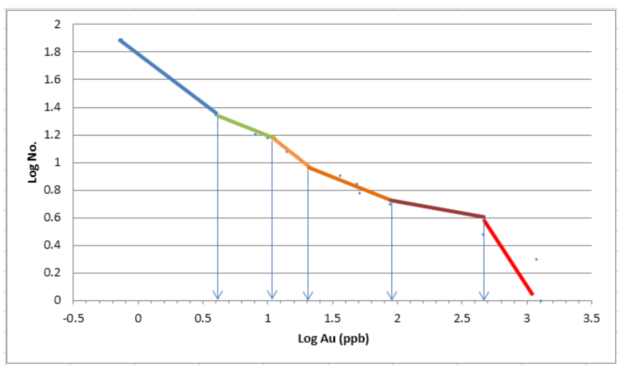

Figure 6. C-N fractal model's Log-log plot based on lithochemical samples.

The results represented that the OAs are 0.97, 0.96, 0.95 and 0.95, respectively (Table 4) and the C–P/A model is the most effective in separating Au anomalies in this region.

Table 4. Overall accuracy (OA) based on the main stream sediment geochemical anomalies obtained through C–P/A, C–N, C–A, C–P fractal models and Au concentrated lithogeochemical samples.

High Intensive Anomalies Obtained by the C–P/A Fractal Model	**High Intensive Lithogeochemical Anomalies**	
	Inside Anomaly	Outside Anomaly
Inside Anomaly	(A)=1	(B)=43
Outside Anomaly	(C)=2	(D)=2189
	Type I error = 0.66	Type II error = 0.98
	Overall accuracy =0.97	

High intensive Anomalies Obtained by the C–N Fractal Model	**High Intensive Lithogeochemical Anomalies**	
	Inside Anomaly	Outside Anomaly
Inside Anomaly	(A)=1	(B)=71
Outside Anomaly	(C)=2	(D)=2161
	Type I error = 0.66	Type II error = 0.96
	Overall accuracy = 0.96	

High Intensive Anomalies Obtained by the C–A Fractal Model	**High Intensive Lithogeochemical Anomalies**	
	Inside Anomaly	Outside Anomaly
Inside Anomaly	(A)=1	(B)=98
Outside Anomaly	(C)=2	(D)=2134
	Type I error = 0.66	Type II error =0. 95
	Overall accuracy = 0.95	

High Intensive Anomalies Obtained by the C–P Fractal Model	**High Intensive Lithogeochemical Anomalies**	
	Inside Anomaly	Outside Anomaly
Inside Anomaly	(A)=1	(B)=98
Outside Anomaly	(C)=2	(D)=2134
	Type I error = 0.66	Type II error = 0.95
	Overall accuracy = 0.95	

In additional, the selected fractal model was evaluded by polymetallic occurrence index (Fig. 7). The results indicated that the OAs is 0.81 (Table 5).

Finally, the main Au anomaly in the western and SW parts of this region was validated by field observations and analysis of collected samples from silicic veins (Fig. 8). There are two collected samples which contain 1.1 ppm and 0.45 ppm. It shows that the main anomaly was determined with high accuracy.

Conclusion

Results obtained by Comparison of the C–P/A, C–N, C–A and C–P fractal models show that the C–P/A model is suitable for the detection of stream sediment anomalies for Au in the Aghkand region. Moreover, the C-A and C-P models are very analogous. The C–P/A fractal model is the proper method with the highest the equal to 0.97.

Furthermore, high intensive Au anomalies were located in the western and southwestern parts of the region.

Table 5. Overall accuracy (OA) based on the main stream sediment geochemical anomalies obtained through C–P/A fractal model and polymetallic occurrence index.

High intensive Anomalies Obtained by the C–N Fractal Model	**Existing polymetallic occurrence index**	
	Inside Anomaly	Outside Anomaly
Inside Anomaly	(A)=7	(B)=2
Outside Anomaly	(C)=159	(D)=691
	Type I error = 0.95	Type II error = 0.99
	Overall accuracy = 0.81	

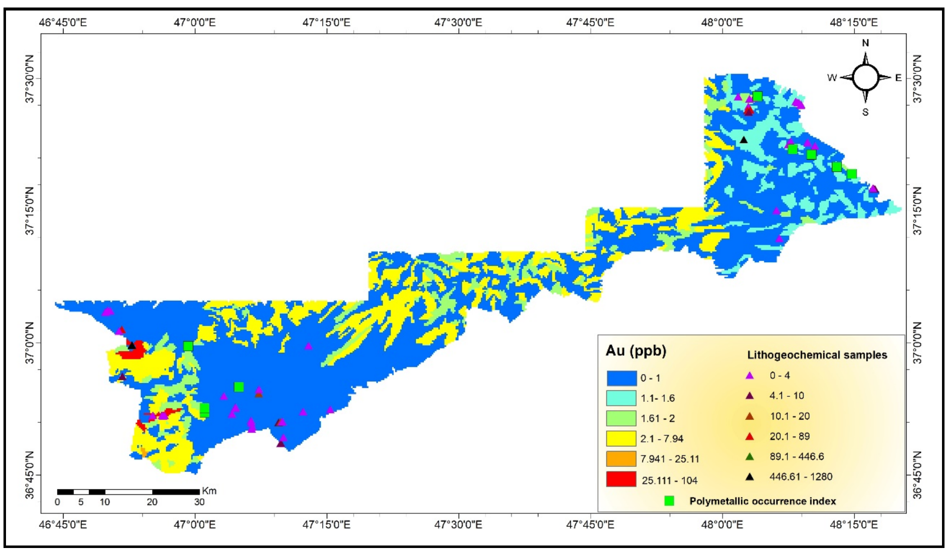

Figure 7. Evaluation map of the distribution of Au by using polymetallic occurrence index.

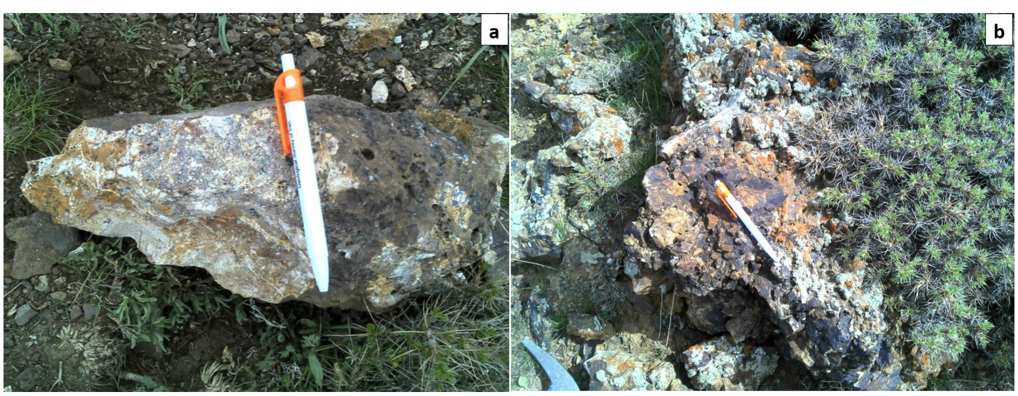

Figure 8. Field observations from silicic veins (a and b).

Ultimately, in order to check the anomalies with a geological map, the situations of stream sediment samples with the catchment basins were studied to find the proper host rocks for gold mineralization. Correspondence between these rock types and the main anomalies indicates that concentration of Au were located in the western and southwestern parts of the study region and were hosted by andesite rocks and tuffs.

References

Agterberg, F., 1995. Multifractal modeling of the sizes and grades of giant and supergiant deposits. International Geology Review, 37: 1–8.

Atapour, H., Aftabi, A, 2007. The geochemistry of gossans associated with Sarcheshmeh porphyry copper deposit, Rafsanjan, Kerman, Iran: Implications for exploration and the environment. Journal Geochemical Exploration, 93: 47–65.

Aliyari, F., Rastad, E., Mohajjel, M., Arehart, G.B., 2009. Geology and geochemistry of DO-C isotope systematics of the Qolqoleh Gold Deposit, Northwestern Iran, implications for ore genesis. Ore Geology Revews, 36: 306–314.

Afzal, P., Khakzad, A., Moarefvand, P., Rashidnejad Omran, N., Esfandiari, B., Fadakar Alghalandis, Y., 2010. Geochemical anomaly separation by multifractal modeling in Kahang (Gor Gor) porphyry system, Central Iran. Journal Geochemical Exploration, 104: 34–46.

Afzal, P., Fadakar Alghalandis, Y., Moarefvand, P., Rashidnejad Omran, N., Asadi Afzal, P., Fadakar Alghalandis, Y., Khakzad, A., Moarefvand, P., Rashidnejad Omran, N., 2011. Delineation of mineralization zones in porphyry Cu deposits by fractal concentration-volume modeling, Journal Geochemical Exploration, 108: 220–232.

Afzal, P., Alhoseini, SH., Tokhmechi, B., Kaveh Ahangaran, D., Yasrebi, A.B., Madani, N., Wetherelt, A., 2014. Outlining of high quality coking coal by concentration–volume fractal model and turning bands simulation in East-Parvadeh coal deposit, Central Iran. International Journal of Coal Geology, 127: 88–99.

Asadi, S., Moore, F., Zarasvandi, A., 2014. Discriminating productive and barren porphyry copper deposits in the southeastern part of the central Iranian volcano-plutonic belt, Kerman region, Iran, A review. Earth-Science Reviews, 138: 25–46.

Afzal, P., Mirzaei, M., Yousefi, M., Adib, A., Khalajmasoumi, M., Zia Zarifi, A., Foster, P., Yasrebi, A., 2016. Delineation of geochemical anomalies based on stream sediment data utilizing fractal modeling and staged factor analysis. Journal of African Earth Sciences, 119: 139–149.

Bölviken, B, Stokke, P.R., Feder, J., Jössang, T., 1992. The fractal nature of geochemical landscapes. Journal Geochemical Exploration, 43: 91–109.

Babaie, H.A., Ghazi, A.M., Babaei, A., La Tour, T.E., Hassanipak, A.A., 2001. Geochemistry of arc volcanic rocks of the Zagros crush zone, Neyriz, Iran. Journal of Asian Earth Science, 19: 61–76.

Cheng, Q., Agterberg, F.P., Ballantyne, S.B., 1994. The separation of geochemical anomalies from background by fractal methods. Journal of Geochemical Exploration, 51: 109–130.

Cheng. Q, 1995. The perimeter area fractal model and its application to geology. Mathematical Geology, 27: 69–82.

Cheng, Q., Xu, Y., Grunsky, E. , 2000. Integrated spatial and spectral analysis for geochemical anomaly separation. Natural Resources Research, 9: 43–52.

Carranza, E.J.M., 2008. Geochemical anomaly and mineral prospectivity mapping in GIS. Handbook of exploration and environmental geochemistry, 11: 1–351.

Carranza, E.J.M., 2009. Controls on mineral deposit occurrence inferred from analysis of their spatial pattern and spatial association with geological features. Ore Geology Reviews, 35: 383–400.

Carranza, E.J.M., 2011. Analysis and mapping of geochemical anomalies using logratio-transformed stream sediment data with censored values. Journal of Geochemical Explortion, 110: 167–185.

Chen, G., Cheng, Q., 2016. Singularity analysis based on wavelet transform of fractal measures for identifying geochemical anomaly in mineral exploration. Computers & Geosciences, 87: 56–66.

Davis, J.C., 2002. Statistics and Data Analysis in Geology, 3rd edition. John Wiley & Sons Inc, New York: 638.

Dargahi. S., Arvin, M., Pan, Y., Babaei, A., 2010. Petrogenesis of post-collisional A-type granitoids from the Urumieh–Dokhtar magmatic assemblage, Southwestern Kerman, Iran, Constraints on the Arabian–Eurasian continental collision. Lithos, 115: 190–204.

Deng, J., Wang, Q., Yang, L., Wang, Y., Gong, Q., Liu, H., 2010. Delineation and explanation of geochemical anomalies using fractal models in the Heqing area, Yunnan Province, China. Journal of Geochemical Exploration, 105: 95–105.

Ellis, A.J., 1979. Explored geothermal systems. In Barnes HL (ed), Geochemistry of hydrothermal ore deposits, 2nd edition, Wiley-Interscience, New York: 632–683.

Ghezelbash, R., Maghsoudi, A., Daviran, M., Yilmaz, H., 2019. Incorporation of principal component analysis, geostatistical interpolation approaches and frequency-space-based models for portraying the Cu-Au geochemical prospects in the Feizabad district, NW Iran. Geochemistry, 79: 323–336.

Ghezelbash, R., Maghsoudi, A., Daviran, M., 2019 a. Combination of multifractal geostatistical interpolation and spectrum–area (S–A) fractal model for Cu–Au geochemical prospects in Feizabad district, NE Iran. Arabian Journal of Geosciences, 12: 152.

Ghezelbash, R., Maghsoudi, A., Carranza, E. J. M., 2019 b. Mapping of single-and multi-element geochemical indicators based on catchment basin analysis: Application of fractal method and unsupervised clustering models. Journal of Geochemical Exploration, 199: 90–104.

Hezarkhani, A., Williams-Jones, A.E., 1998. Controls of alteration and mineralization in the Sungun porphyry copper deposit, Iran, evidence from fluid inclusions and stable isotopes. Economic Geology, 93: 651–670.

Haroni, H., 2012. Application of power-spectrum-volume fractal method for detecting hypogene, supergene enrichment, leached and barren zones in Kahang Cu porphyry deposit, Central Iran. Journal Geochemical Exploration, 112: 131–138.

Heidari, S.M., Ghaderi. M., Afzal, P., 2013. Delineating mineralized phases based on lithogeochemical data using multifractal model in Touzlar epithermal Au–Ag (Cu) deposit, NW Iran. Geochemistry, 31: 119–132.

Karimzadeh Somarin, A., 2005. Petrology and geochemistry of Early Tertiary volcanism of the Mendejin area, Iran, and implications for magma genesis and tectonomagmatic setting. Geodinamic Acta, 18: 343–362.

Karimzadeh Somarin, A., 2006. Geology and geochemistry of the Mendejin plutonic rocks, Mianeh, Iran. Journal of Asian Earth Sciences, 27: 819–834.

Karimzadeh Somarin., A., Lentz, D.R., 2008. Mineralogy, geochemistry and fluid evolution of a fossil hydrothermal system in the Paleogene Mendejin volcanic sequence, East Azarbaijan, Iran. Mineralogy and Petrology, 94: 123–143.

Li, C., Ma., T., Shi., J., 2003. Application of a fractal method relating concentrations and distances for separation of geochemical anomalies from background. Journal of Geochemical Exploration, 77: 167–175.

Lotfi, M., Karimi, M., 2004. Mineralization and genesis of vein type Baycheh Baq deposit (Zanjan, NW Iran), Ulum-I-Zamin, 53: 40–55 (In Persian).

Mandelbrot, B.B., 1983. The fractal geometry of nature. W.H. Freeman and company, San Francisco: 468.

Mohajjel, M., Fergusson, C.L., 2000. Dextral transpression in Late Cretaceous continental collision, Sanandaj-Sirjan zone, western Iran. Journal of Structural Geology, 22: 1125–1139.

Maghsoudi., A., Rahmani, M., Rashidi, B., 2005. Gold deposites and indications of iran. Research manual for Students of Earth Science (In Persian).

Yousefi, M., Carranza, E.J., Kamkar-Rouhani, A., 2013. Weighted drainage catchment basin mapping of geochemical anomalies using stream sediment data for mineral potential modeling. Journal of Geochemical Exploration, 128: 88-96.

Makovicky, E., Topa, D., Tajeddin, H., Putz, H., Zagler, G., 2013. Ferdowsiite a new mineral from the Barika ore deposit, Iran. Candian Mineralogist, 51: 727–734.

Pirajno, F., 2009. Hydrothermal Processes and Mineral Systems. Springer, The University of Western Australia, Perth.

Parsa. M., Maghsoudi, A., Ghezelbash, R., 2016. Decomposition of anomaly patterns of multi-element geochemical signatures in Ahar area, NW Iran, a comparsion of U-spatial statistic and fractal models. Arabian Journal of Geoscience, 9: 260.

Parsa, M., Maghsoudi, A., Yousefi, M., Carranza. E.J.M., 2017. Multiftactal interpolation and sediment geochemical data: Implication for mapping exploration targets. Journal of African Earth Sciences, 128: 5–15.

Sim, B.L., Agterberg, F.P., Beaudry, C., 1999. Determining the cutoff between backgroundand relative base metal contamination levels using multifractal methods. Computers and Geosciences, 25: 1023–1041.

Shen, W., Zhao, P., 2002. Theoretical study of statistical fractal model with applications to mineral resource prediction, Computer and Geosciences, 28: 369–376.

Shafiei, B., Haschke, M., Shahabpour, J., 2009. Recycling of orogenic arc crust triggers porphyry Cu mineralization in Kerman Cenozoic arc rocks, southeastern Iran. Mineralium Deposita, 44: 265–283.

Sadeghi, B., Moarefvand, P., Afzal, P., Yasrebi, A.B., Daneshvar, Saein, L., 2012. Application of fractal models to outline mineralized zones in the Zaghia iron ore deposit, Central Iran. Journal of Geochemical Exploration, 122: 9–19.

Sadeghi, B., Madani, N., Carranza, E.J.M., 2015. Combination of geostatistical simulation and fractal modeling for mineral resource classification. Journal of Geochemical Exploration, 149: 59–73.

Tajeddin, H., 2011. Gold ore controlling factors in metamorphic rocks of Saqez–Sardasht, NW of Sananda–Sirjan metamorphic zone. Ph.D. Dissertation, Tarbiat Modarres University, Tehran, Iran: 436.

Zarasvandi, A., Rezaei, M., Raith, J., Lentz, D., Azimzadeh, A.M., Pourkaseb H., 2015. Geochemistry and fluid characteristics of the Dalli porphyry Cu–Au deposit, Central Iran. Journal of Asian Earth Sciences, 111: 175–191.

Zuo, R., Wang, J., Chen, G., Yang, M., 2015. Identification of weak anomalies: A multifractal perspective. Journal of Geochemical Exploration, 148: 12–24.